

We are IntechOpen, the world's leading publisher of Open Access books Built by scientists, for scientists

6,000

Open access books available

148,000

International authors and editors

185M

Downloads

Our authors are among the

154

Countries delivered to

TOP 1%

most cited scientists

12.2%

Contributors from top 500 universities



WEB OF SCIENCE™

Selection of our books indexed in the Book Citation Index
in Web of Science™ Core Collection (BKCI)

Interested in publishing with us?
Contact book.department@intechopen.com

Numbers displayed above are based on latest data collected.
For more information visit www.intechopen.com



Ascorbic Acid-assisted Green Synthesis of Silver Nanoparticles: pH and Stability Study

Katherine Guzmán, Brajesh Kumar, Marcelo Grijalva, Alexis Debut and Luis Cumbal

Abstract

In this chapter, eco-friendly *in situ* synthesis of silver nanoparticles (AgNPs) using a mixture of ascorbic acid and citric acid is introduced. The synthesis conditions of the AgNPs were optimized by adjusting the pH of the reaction mixture. Different spectroscopic and microscopic techniques have been used to characterize the physico-chemical properties of AgNPs. The synthesis of AgNPs was primarily identified by the appearance of yellow colour and confirmed by showing $\lambda_{\max} = 409$ nm in UV-visible spectroscopy. All characterization techniques reveal that the generated AgNPs were non-aggregated, quasi-spherical shapes with an average size of 22.4 ± 13.2 nm, and face-centred cubic crystalline structures. Infrared spectroscopy confirms the surface of AgNPs covered with -COOH group and shows peaks at 1733, 1759, 3262 and 3633 cm^{-1} . Moreover, synthesized AgNPs at pH 10 were stable for one month with a slight change in size. A straightforward, facile and environmentally-friendly synthesis of highly stable AgNPs may contribute to future engineering applications.

Keywords: green synthesis, silver nanoparticles, ascorbic acid, TEM, UV-Vis spectroscopy

1. Introduction

Nanotechnology's ability to design and manipulate matter at an atomic scale has been encouraging over the last few decades. Being a source of novel products that need to be beneficial for the environment, the metal nanoparticles (MNPs) displayed an unusual characteristics that make them valuable. Metals like silver include remarkable optical and chemical properties in which the synthesis of silver nanoparticles (AgNPs) highly depends on controlling the size, shape, crystallinity, composition and several features ruled by the unique effects of nanobiotechnology [1, 2]. Silver is the most promising metal due to the bactericidal potential used since ancient times and unique properties such as high thermal stability [3]. AgNPs have diverse applications such as environmental protection, catalysis, food industries, medicine and others [4].

However, hazardous and environmentally unfriendly conditions are not demanded to apply for the synthesis of nanomaterial. The protocols followed to synthesize AgNPs should be feasible, cleaner, long-lasting, low-cost and safer. In other words, the green synthesis of AgNPs does not require any physical, electrical or modification processes [5]. In recent years, researchers have been interested to control and improve engineering procedures of the desired nanoparticle features [6]. Some experts have suggested that the AgNPs synthesis key relates to the selection of right parameters that permit the control over the size and shape outcomes [7].

Numerous scientific articles in the field of AgNPs synthesis have been published, and most of the traditional methods are based on the *bottom-up* category such as chemical reduction, light assisted, sol-gel, electrochemical method, etc [8, 9]. Green synthesis of AgNPs using a variety of reducing-stabilizing agent includes gallic acid-chitosan [10], cellulose [11], gelatin [12], starch [13], ascorbic acid [14], quercetin [15], sodium citrate [16], ascorbic acid-gelatin [17], ascorbic acid-sodium dodecyl sulphate [18], tannic acid-sodium citrate [19], plant extracts [20], etc have been reported.

In this study, the *bottom-up* strategy was used to synthesize AgNPs using ascorbic acid as a reductive agent and citric acid as a potent complex stabilizer, effectively. We also looked at the effect of pH on stable AgNPs colloid formation and the particle size. Furthermore, various spectroscopic and microscopic techniques were used to characterize the physicochemical properties of AgNPs.

2. Experimental

2.1 Chemicals

Silver nitrate (AgNO_3 , 99%) was obtained from Sigma-Aldrich, Germany. Ascorbic acid ($\text{C}_6\text{H}_8\text{O}_6$, 99%, powder/USP/FCC) and sodium hydroxide (NaOH) were purchased from Fisher Chemical, China. Trisodium citrate ($\text{Na}_3\text{C}_6\text{H}_5\text{O}_7$, 99%) was acquired from Loba Chemie, India.

2.2 Preparation of AgNPs

The formation of AgNPs from ascorbic acid and sodium citrate was monitored by a colour change in the reaction medium [21]. The final adapted solution for the preparation of the AgNPs was 20 mL of ascorbic acid (0.6 mM) and 20 mL of sodium citrate (3 mM). Before preparation of AgNPs, the pH of these solutions was adjusted to 9, 10 and 11 by the addition of 0.1 M NaOH in a separate flask. One flask was stored as a control (pH = 6.7). Subsequently, 4 mL of 1 mM of AgNO_3 was added to each flask under stirring conditions in the water bath at 60–65°C for two hours. Each reaction mixture containing AgNPs was diluted seven times and analyzed in the UV-visible spectrophotometer.

2.3 Characterization of AgNPs

Formation and stability of AgNPs were determined by a UV-visible spectrophotometer, SPECORD® S600 from Analytik Jena, Germany. The mean particle size and stability were analyzed in a dynamic light scattering (DLS) instrument (HORIBA, LB-550 Japan). The shape, size and selected area electron diffraction (SAED) pattern

of AgNPs were captured from transmission electron microscopy, TEM (FEI Tecnai, G2 Spirit Twin, Holland). X-ray diffraction (XRD) analyses were performed with a PANalytical brand θ - 2θ configuration (generator-detector) x-ray tube, copper $\lambda = 1.54059 \text{ \AA}$ and EMPYREAN diffractometer. The Fourier transform infrared spectroscopy (FTIR) measurements were performed on a Spectrum 100 IR spectrometer (Perkin Elmer, USA) using the attenuated total reflectance (ATR) technique to determine the possible involvement of functional groups in the synthesis of nanoparticles.

3. Results and discussion

3.1 Visual and UV-vis spectroscopy studies

The initial synthesis of AgNPs was assessed through visual colour and UV-Vis spectrometric analysis. After the addition of AgNO_3 to the alkaline reaction mixture, the colour becomes yellowish within 5 mins, showing the reduction of Ag^+ to Ag^0 and the formation of AgNPs [22]. Detection of UV-visible peak between 390 and 410 nm implies the presence of small and spherically shaped AgNPs [23]. Mie [24] said that only one surface plasmonic resonance (SPR) band produces spherical nanoparticles, while two or more SPR bands cause shape variation. The colour arises in nanoparticles due to SPR, a non-linear optical property related to the excitation of electrons and collective oscillation of dipoles under the influence of electromagnetic field of light [2]. Kumar et al., 2014 observed similar SPR result in UV-vis absorption spectroscopy using *Plukenetia volubilis* leaf extracts [25].

The SPR band can provide useful information about the morphology and particle distribution of the synthesized nanoparticles. In order to understand the effect of pH in the synthesis of AgNPs, we performed the reaction at different pH levels (**Figure 1**). The reaction mixture showed a sharp absorption band at pH 9, 10 and 11, while no band was observed at pH 6.7. The SPR band observed for pH 10 was narrower than others (pH = 9 and 11). It clearly showed a narrow size distribution of AgNPs at pH 10 and was more selective [26]. The cause behind this observation was that at $\text{pH} > 9$, free H^+ of ascorbic acid and citric acid are consumed, and the amount of free OH^- increases. In **Figure 2**, the maximum absorption band (λ_{max}) for AgNPs at pH 10 was 409 nm and λ_{max} observed at pH 11 was 404 nm, respectively. Synthesis of AgNPs at pH 10 provides a narrow absorption band and seems to be a uniform size distribution. After 4 weeks, its absorption band increases slightly and shifted towards shorter wavelengths (408 nm and 406 nm), which is a typical characteristic of smaller nanoparticles. The redox potential of ascorbic acid depends on the pH, when the pH increases, the redox potential decreases. Increased difference of redox potentials between Ag^+ and the ascorbic acid/ reducing agent makes the reaction faster, and smaller AgNP nuclei are created [14]. The reduction of Ag^+ ions is difficult due to the complex formation with citrate and results in greater stability through the outer surface coverage [27, 28].

To monitor the stability of the AgNPs prepared at pH 10, the SPR absorption spectra of the AgNPs (stored at $23\text{--}25^\circ\text{C}$) were measured for 7, 14, 21 and 28 days (**Figure 3**). At various incubation periods, a slight increase in the intensity of the SPR peaks was observed. In addition, λ_{max} for the SPR peaks of AgNPs have almost remained constant. It clearly explained that the reaction mixture having a pH at 10 is most appropriate to reduce Ag^+ ions into AgNPs and stable over a month. These

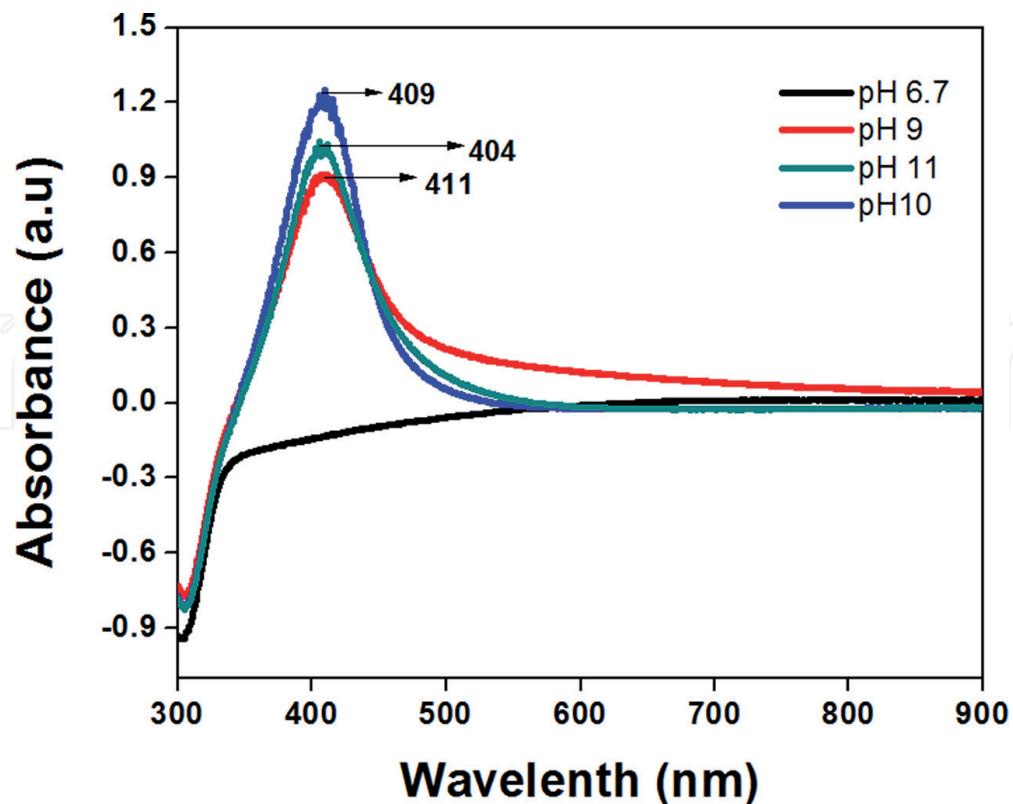


Figure 1.
UV-vis spectrum of AgNPs synthesized at different pH.

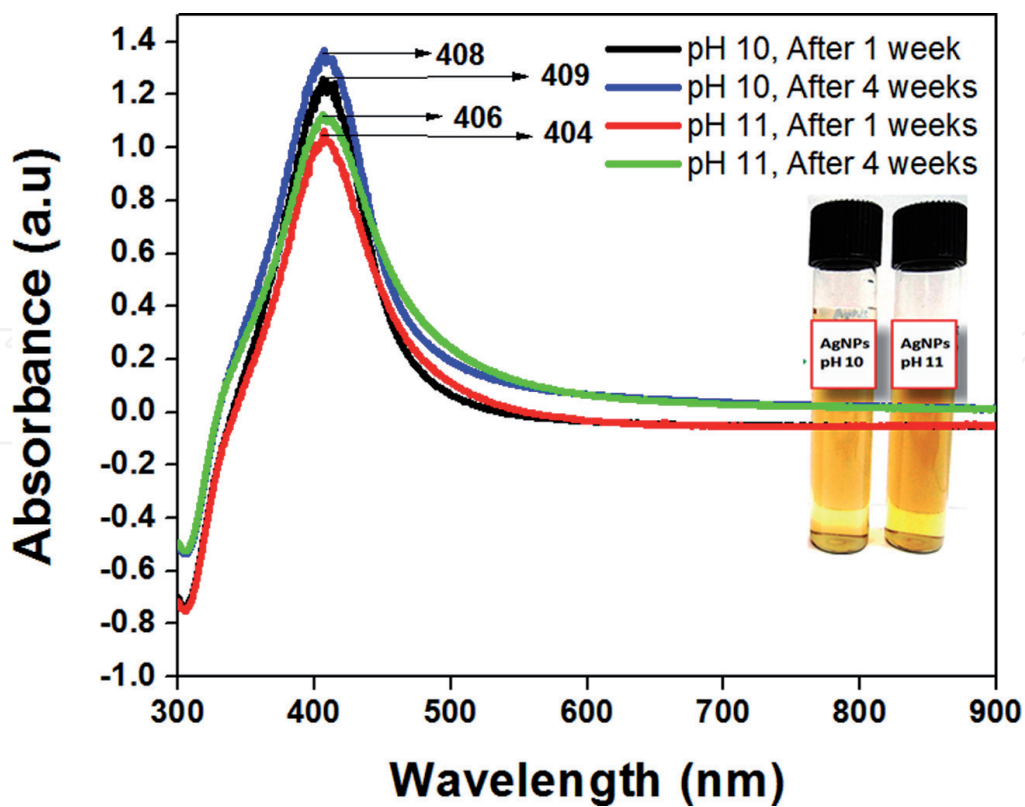


Figure 2.
UV-vis spectrum of AgNPs synthesized at pH 10 and 11 for different incubation times [Inset: visual image of AgNPs synthesized at pH 10 and 11].

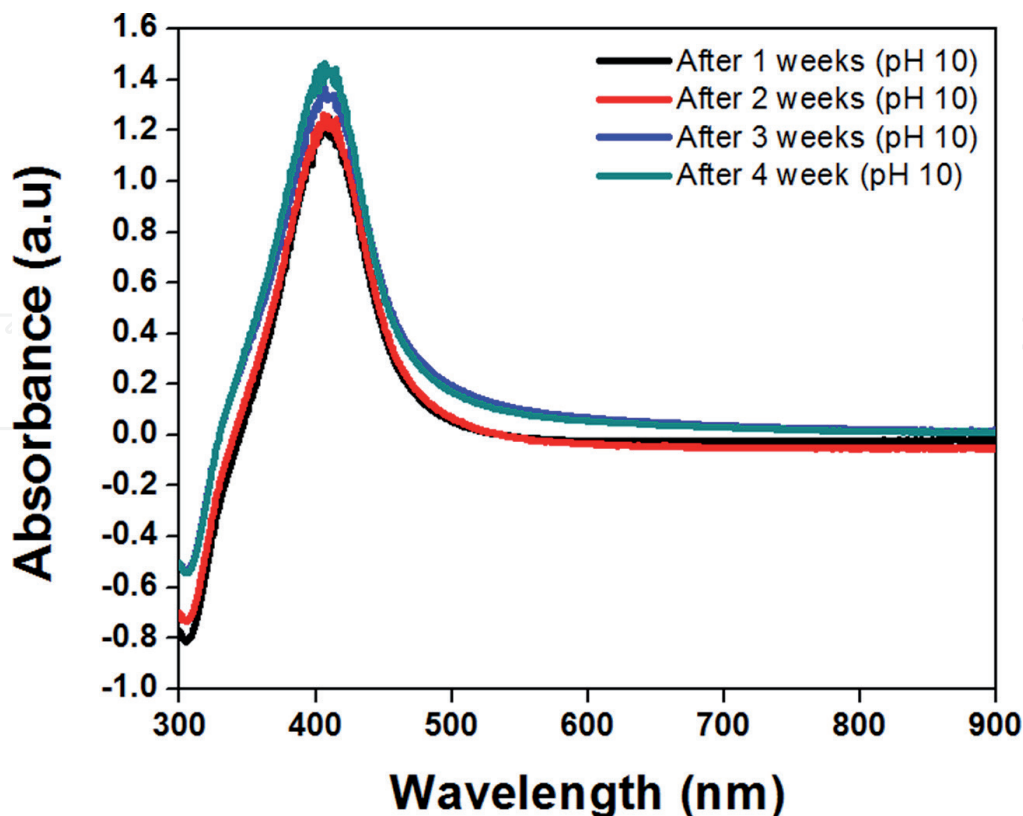
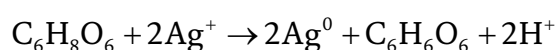


Figure 3.
UV-vis spectrum of AgNPs synthesized at pH 10 and different incubation times.

findings were further confirmed by the DLS analysis. The reduction of Ag^+ ions by ascorbic acid ($\text{C}_6\text{H}_8\text{O}_6$) was suggested as follows [28]:



3.2 DLS and TEM analysis

DLS tests are performed to investigate the size distribution and stability of the colloidal AgNPs in the aqueous medium. As shown in **Figure 4**, the mean size of the AgNPs synthesized at a pH of 10 over 7 days is 22.4 ± 13.2 nm and the observed polydispersity index (PDI) is 0.3472. $\text{PDI} > 0.1$ confirms the polydispersed nature of nanoparticles in the aqueous phase [2, 10]. These findings were summarized and correlated by the UV-Vis and DLS analysis mentioned in **Table 1**. The DLS data of reaction mixture at pH 10 ($\lambda_{\text{max}} = 409$ nm) directly indicated that smaller particles were formed with respect to other pH levels. Hence, pH 10 was preferred for the synthesis of stable and smaller diameter particles. This result agrees with UV-vis and TEM results.

In **Figure 5a** and **b**, TEM image clearly showed the presence of non-aggregated and monodisperse AgNPs of an average size of 30 nm. Furthermore, the low magnification TEM images confirm the uniform size and quasi-spherical shape of AgNPs. Slight change in mean size observed in TEM and DLS analysis may be due to the

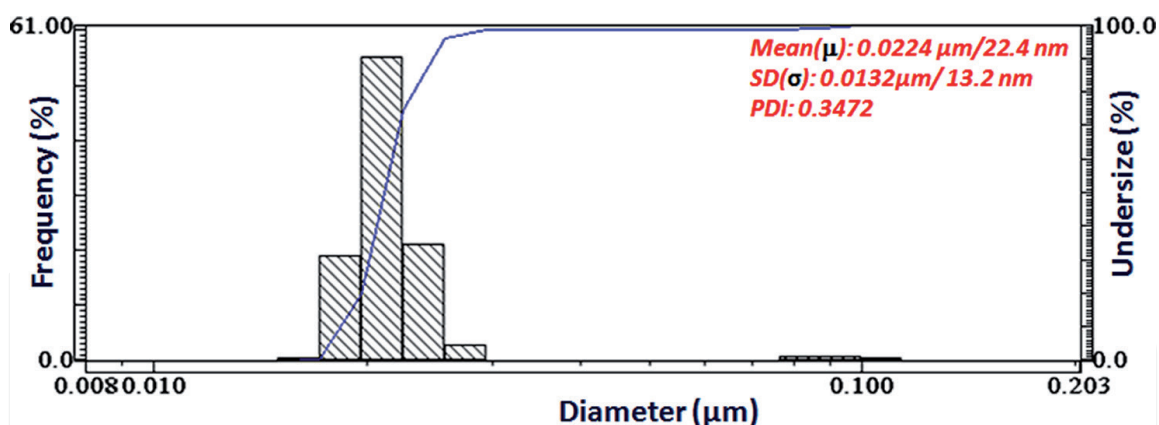


Figure 4.
DLS pattern of AgNPs synthesized at pH 10 for 1st week.

pH of reaction mixture	Particles diameter ($\mu \pm \sigma$) nm	Particles diameter ($\mu \pm \sigma$) nm	Particles diameter ($\mu \pm \sigma$) nm	Particles diameter ($\mu \pm \sigma$) nm	UV-vis λ_{\max} (nm)
	Time: 1st week	Time: 2nd week	Time: 3rd week	Time: 4th week	
6.7	117.72 \pm 54.3	125.7 \pm 203.3	156.5 \pm 55.9	158.75 \pm 60.3	No sharp peak
9	49.9 \pm 59.9	45.34 \pm 39.2	59.9 \pm 33.4	67.3 \pm 33.9	411
10	22.4 \pm 13.2	23.1 \pm 13.3	25.2 \pm 13.9	29.1 \pm 11.1	409
11	28.7 \pm 17.6	32.2.7 \pm 18.1	30.1 \pm 16.5	32.3 \pm 14.3	404

Table 1.
Particle mean diameter and UV-vis values for different pHs and time intervals.

presence of some impurity in the sample or screening of small particles by bigger ones in the DLS analysis [29]. The SAED pattern of ascorbic acid-induced AgNPs is illustrated in **Figure 5c**. The concentric ring-like diffraction pattern in the SAED pictures clearly indicates that the particles are polycrystalline and spherically shaped [23, 25].

3.3 XRD and FTIR analysis

The crystal structure of the nanoparticles was confirmed with the help of the XRD technique. The XRD profile of the AgNPs synthesized by ascorbic acid and sodium citrate at pH 10 is presented in **Figure 6**. The presence of an intense peak at 38.0696° corresponds to (111) planes and indicates the growth of AgNPs along the (100) directions, while another peak at 44.2506° indexed as (200) reflection plane of metallic silver, respectively (ICSD no: 98-018-0878). The presence of an unindexed peak at $2\theta = 31.6858^\circ$ in the XRD profile indicates the organic/ bioinorganic impurities [8, 10]. These observations confirmed the successful formation of the semicrystalline AgNPs and also justify the outcomes of the SAED.

FTIR spectrum analysis is crucial to describe the processes that take place during AgNPs synthesis. The characteristic bands observed at 1759 and 1733 cm^{-1} correspond to the C=O stretching of citric acid, whereas the presence of C=O stretching vibration at 1653 cm^{-1} confirms the oxidized form of ascorbic acid [19]. The presence of 1559 and 1383 cm^{-1} is characteristic of C=O asymmetric stretching in the $-\text{COO}^-$ and

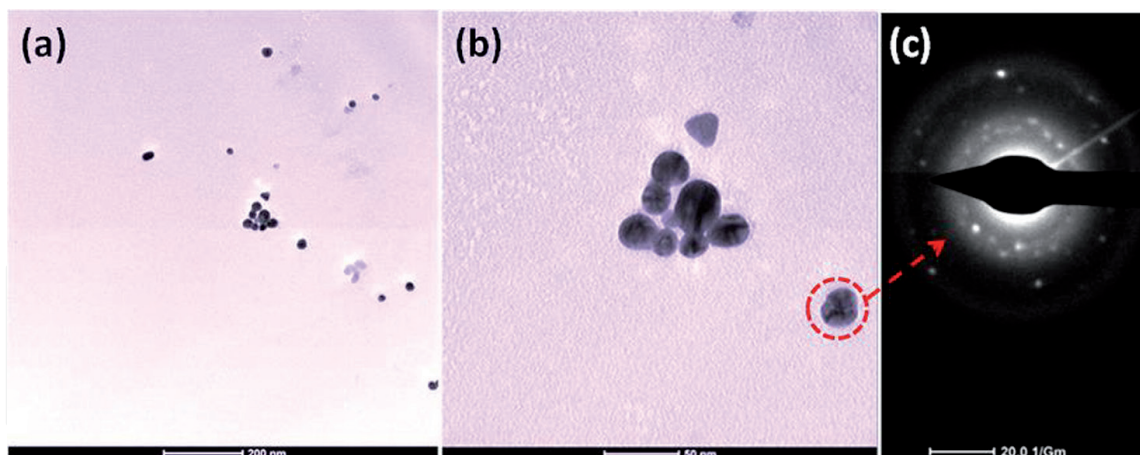


Figure 5.
(a,b) TEM image and corresponding (c) SAED pattern of AgNPs.

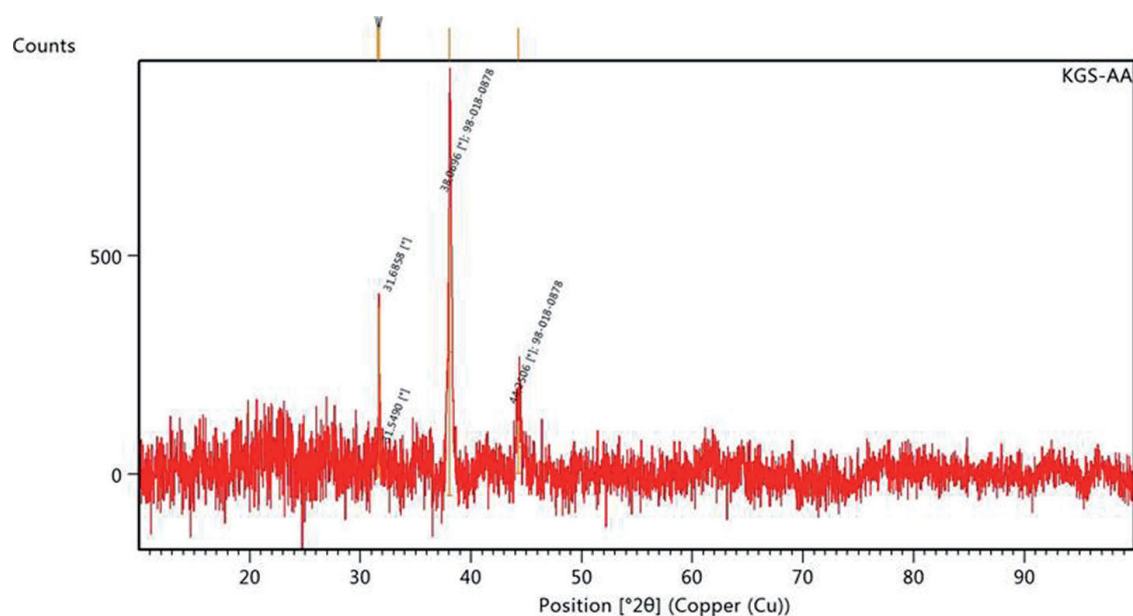


Figure 6.
XRD pattern of AgNPs synthesized by a mixture of ascorbic acid and sodium citrate.

C–OH stretching peaks of citric acid. Both –O–H (multiple) and C–O–C stretch vibration is detected at 3885, 3810, 3633, 3262 cm^{-1} and 1049 cm^{-1} represented for ascorbic acid and organic/citric acid (**Figure 7**) [23]. Furthermore, the bands at 1462 cm^{-1} correspond to C–H bending and CH_2 scissoring of the aliphatic group, while peaks occurred at 915 cm^{-1} for alkenes and 830 cm^{-1} for –OH out of plane deformation/C–C ring stretching. The FTIR results indicate that the citric acid is directly involved in the stabilization and capping of AgNPs, whereas ascorbic acid reduces Ag^+ ions to Ag^0 . The UV-vis, TEM and XRD data justify the FTIR analysis statement.

4. Conclusions

In conclusion, the combined use of ascorbic acid and sodium citrate was proposed as a simple and non-toxic method for the green synthesis of AgNPs because it permits

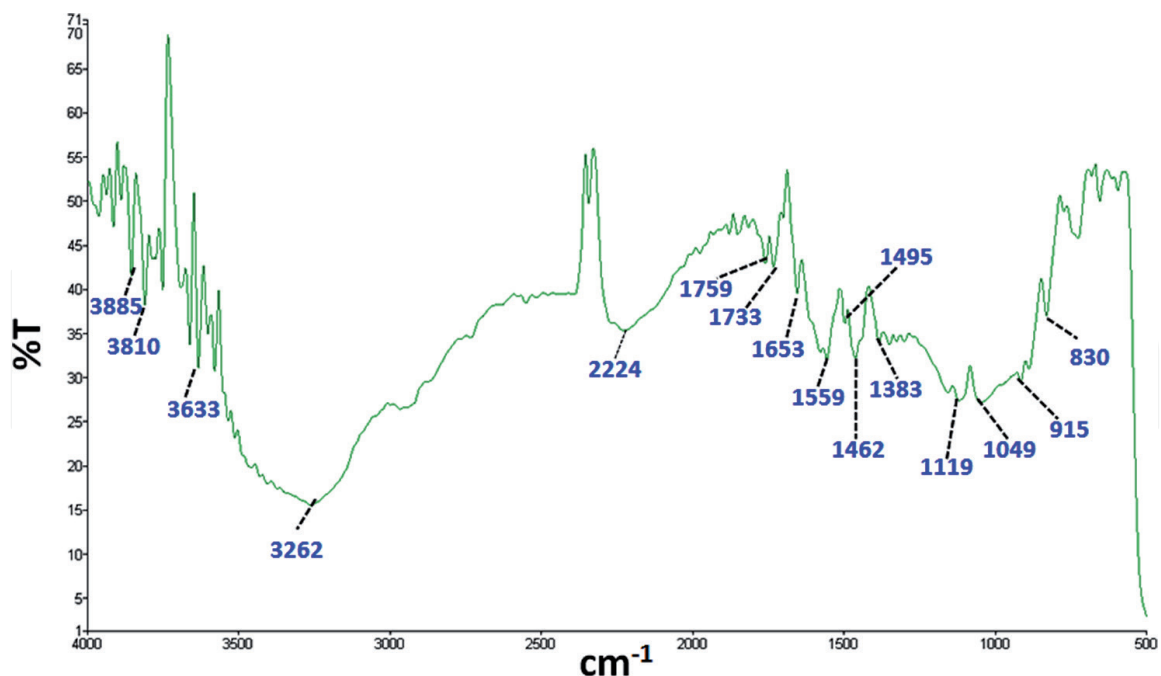


Figure 7.
FTIR pattern of AgNPs synthesized by ascorbic acid and sodium citrate.

the control of the nucleation, growth and stabilization of the synthesis process. It shows $\lambda_{\text{max}} = 409 \text{ nm}$ at pH 10 and produces monodisperse, quasi-spherical shape AgNPs with an average size of 30 nm under optimized conditions. Additionally, AgNPs were stable for one month, the XRD result confirms that the crystallinity of AgNPs is FCC in nature and FTIR suggested capping of AgNPs by $-\text{COO}^-$ group of sodium citrate. Therefore, the suggested environmentally-friendly synthesis of AgNPs will contribute to the future engineering applications.

Acknowledgements

This scientific work has been funded by the Universidad de las Fuerzas Armadas ESPE and Prometeo Project of the National Secretariat of Higher Education, Science, Technology and Innovation (SENESCYT), Ecuador.

Conflict of interest

The authors confirm they have no conflict of interest.

IntechOpen

Author details


Katherine Guzmán¹, Brajesh Kumar^{1,2*}, Marcelo Grijalva¹, Alexis Debut¹
and Luis Cumbal¹

1 Centro de Nanociencia y Nanotecnología, Universidad de las Fuerzas Armadas ESPE, Sangolqui, Ecuador

2 Department of Chemistry, TATA College, Kolhan University, Chaibasa, Jharkhand, India

*Address all correspondence to: krmbraj@gmail.com

IntechOpen

© 2022 The Author(s). Licensee IntechOpen. This chapter is distributed under the terms of the Creative Commons Attribution License (<http://creativecommons.org/licenses/by/3.0>), which permits unrestricted use, distribution, and reproduction in any medium, provided the original work is properly cited. 

References

- [1] Singh OV. Bio-nanoparticles: Biotechnological Applications. New Jersey: John Wiley & Sons; 2015
- [2] Kumar B, Smita K, Angulo Y, Debut A, Cumbal L. Single-step biogenic synthesis of silver nanoparticles using honeybee-collected pollen. *Inorganic and Nano-Metal Chemistry*. 2022. DOI: 10.1080/24701556.2022.2081198
- [3] Gebauert J, Malissek J, Sonja S, Knauer S, Maskos M, Stauber M, et al. Impact of the nanoparticle–protein corona on colloidal stability and protein structure. *Langmuir*. 2012;**28**(25):9673-9679
- [4] Singh M, Manikandan S, Kumaraguru AK. Nanoparticles: A new technology with wide applications. *Research Journal of Nanoscience and Nanotechnology*. 2010;**1**(1):1-11
- [5] Lok C, Chi-Ming L, Rong C, He Q, Yu Y, Sun H, et al. Silver nanoparticles: Partial oxidation and antibacterial activities. *Journal of Biological Inorganic Chemistry*. 2007;**12**:527-534
- [6] Burda C, Chen X, Narayanan R, Mostafa A, Sayed E. Chemistry and properties of nanocrystals of different shapes. *Chemical Review*. 2005;**105**(4):1025-1102
- [7] Sönnichsen C, Reinhard M, Liphardt J, Alivisatos AP. A molecular ruler based on plasmon coupling of single gold and silver nanoparticle. *Nature Biotechnology*. 2005;**23**(6):741-745
- [8] Kumar B, Smita K, Cumbal L, Debut A. *Ficus carica* (Fig) fruit mediated green synthesis of silver nanoparticles and its antioxidant activity: A comparison of thermal and ultrasonication approach. *BioNanoScience*. 2016;**6**:15-21
- [9] Pacioni NL, Borsarelli CD, Rey R, Veglia AV. *Synthetic Routes for the Preparation of Silver Nanoparticles*. Switzerland: Springer International Publishing; 2015
- [10] Guzmán K, Kumar B, Vallejo MJ, Grijalva M, Debut A, Cumbal L. Ultrasound-assisted synthesis and antibacterial activity of gallic acid-chitosan modified silver nanoparticles. *Progress in Organic Coatings*. 2019;**129**:229-235
- [11] Mochochoko T, Oluwafemi OS, Jumbam DN, Songca SP. Green synthesis of silver nanoparticles using cellulose extracted from an aquatic weed; water hyacinth. *Carbohydrate Polymers*. 2013;**98**:290-294
- [12] Kanmani P, Rhim J-W. Physicochemical properties of gelatin/silver nanoparticle antimicrobial composite films. *Food Chemistry*. 2014;**148**:162-169
- [13] Kumar B, Smita K, Cumbal L, Debut A, Pathak RN. Sonochemical synthesis of silver nanoparticles using starch: A comparison. *Bioinorganic Chemistry and Applications*. 2014;**2014**:8. DOI: 10.1155/2014/784268
- [14] Malassis L, Dreyfus R, Murphy RJ, Hough LA, Donnio B, Murray, CB. One-step green synthesis of gold and silver nanoparticles with ascorbic acid and their versatile surface post-functionalization. *RSC Advances*. 2016;**6**:33092-33100
- [15] Egorova M, Revina AA. Synthesis of metallic nanoparticles in reverse micelles

in the presence of quercetin. *Colloids and Surfaces A: Physicochemical and Engineering Aspects*. 2000;**168**:87-96

[16] Li H, Xia H, Ding W, Li Y, Shi Q, Wang D, et al. Synthesis of monodisperse, quasi-spherical silver nanoparticles with sizes defined by the nature of silver precursors. *Langmuir*. 2014;**30**(1):2498-2504

[17] Chekin F, Ghasemi S. Silver nanoparticles prepared in presence of ascorbic acid and gelatin, and their electrocatalytic application. *Bulletin Material Science*. 2014;**37**(6):1433-1437

[18] Rastegarzadeh S, Hashemi F. A surface plasmon resonance sensing method for determining captopril based on in situ formation of silver nanoparticles using ascorbic acid. *Spectrochimica Acta Part A: Molecular and Biomolecular Spectroscopy*. 2014;**122**:536-541

[19] Ranoszek-Soliwoda K, Tomaszewska E, Socha E, Krzyczmonik P, Ignaczak A, Orłowski P, et al. The role of tannic acid and sodium citrate in the synthesis of silver nanoparticles. *Journal of Nanoparticle Research*. 2017;**19**:273

[20] Kumar B. Green synthesis of gold, silver, and iron nanoparticles for the degradation of organic pollutants in wastewater. *Journal of Composite Science*. 2021;**5**:219. DOI: 10.3390/jcs5080219

[21] Kim D-Y, Sung JS, Kim M, Ghodake G. Rapid production of silver nanoparticles at large-scale using gallic acid and their antibacterial assessment. *Materials Letters*. 2015;**155**:62-64

[22] Stamplecoskie K. Silver Nanoparticles: From Bulk Material to Colloidal Nanoparticles. In: Alarcon E,

Griffith M, Udekwu K, editors. *Silver Nanoparticle Applications*. Engineering Materials. Vol. 1. Cham: Springer; 2015. pp. 1-12. DOI: 10.1007/978-3-319-11262-6

[23] Kumar B, Smita K, Debut A, Cumbal L. Extracellular green synthesis of silver nanoparticles using Amazonian fruit Araza (*Eugenia stipitata* McVaugh). *Transactions on Nonferrous Metals*. 2016;**26**:2363-2371

[24] Mie G. Contribution to the optical properties of turbid media, in particular of colloidal suspensions of metals. *Annals of Physics (Leipzig)*. 1908;**25**:377-452

[25] Kumar B, Smita K, Cumbal L, Debut A. Synthesis of silver nanoparticles using Sacha inchi (*Plukenetia volubilis* L.) leaf extracts. *Saudi Journal of Biological Sciences*. 2014;**21**(6):605-609

[26] Vigneshwaran N, Nachane RP, Balasubramanya RH, Varadarajan PV. A novel one-pot 'green' synthesis of stable silver nanoparticles using soluble starch. *Carbohydrate Research*. 2006;**341**:2012-2018

[27] Dadosh T. Synthesis of uniform silver nanoparticles with a controllable size. *Materials Letter*. 2009;**63**:2236-2238

[28] Singha D, Barman N, Sahu K. Facile synthesis of high optical quality silver nanoparticles by ascorbic acid reduction in reverse micelles at room temperature. *Journal of Colloid and Interface Science*. 2014;**413**:37-42

[29] Kumar B, Smita K, Awasthi SK, Debut A, Cumbal L. *Capsicum baccatum* (Andean Chilli)-assisted phytosynthesis of silver nanoparticles and their H₂O₂ sensing ability. *Particulate Science and Technology*. 2022;**40**(6):772-780